Appendix:
Toward a Radiometric Ice Clock: Uranium Ages of the Dome C Ice Core

Sarah M. Aciego[a,b,*], Bernard Bourdon[a,c], Jakob Schwander[d], Heinrich Baur[a], Alessandro Forieri[e]

[a] *Institute of Geochemistry and Petrology, ETH Zurich, Switzerland.*
[b] *now at Department of Geological Sciences, University of Michigan, Ann Arbor, MI*
[c] *now at Ecole Normale Suprieure de Lyon, CNRS, Lyon, France*
[d] *Climate and Environmental Physics, Physics Institute, University of Bern, Switzerland.*
[e] *Istituto Nazionale di Geofisica e Vulcanologia, Via di Vigna Murata 605, Roma, Italy.*

A.1. ^{234}U Recoil-Accumulation Age Equation

U-series ages determined from recoil products from dust into ice are determined based on the following age equations:

$^{234}U_{ice}$, *no initial component, from Fireman (1986)*

$$\lambda_{234}U_{234}^{ice} = f\lambda_{238}U_{238^{dust}}\left(1 - e^{-\lambda_{234}t}\right) \tag{1a}$$

$$t = \left(-\frac{1}{\lambda_{234}}\right)\ ln\left[1 - \left(\frac{\lambda_{234}U_{234}}{\lambda_{238}U_{238}}\right)\left(\frac{1}{f}\right)\right] \tag{1b}$$

This assumes that the amount of uranium present in the initial precipitation (snow) is so small as to be negligible. This equation is similar to the equation for uranium-recoil comminution ages for small grains (Lee et al., 2010). An activity equation that takes into account initial U is as follows.

*Corresponding author; aciego@umich.edu

10 $^{234}U_{ice}$, *initial component*

The activity of ^{234}U in the ice is due to (1) the recoil out of the dust plus (2) the decaying initial ^{234}U dissolved in the precipitation plus (3) the accumulation from the decay of ^{238}U dissolved in the precipitation. Part (1) is just Equation 1a, above, and parts (2) and (3) are daughter-decay and daughter-accumulation equations that are readily available in isotope geochemistry textbooks such as Faure and Mensing (2004) or Dickin (2005). The resulting equation that combines (1), (2) and (3) is:

$$\lambda_{234}U_{234}^{ice} \;=\; f\lambda_{238}U_{238}^{dust}\left(1-e^{-\lambda_{234}t}\right) \;+\; \lambda_{234}U_{234}^{in}\,e^{-\lambda_{234}t} \;+\; \lambda_{238}U_{238}^{ice}\left(1-e^{-\lambda_{234}t}\right) \quad (2)$$

Rearranging and solving for t results in the recoil age:

$$t \;=\; -\left(\frac{1}{\lambda_{234}}\right)\; ln\left(\frac{[U_{234}]_{ice}-f\,[U_{238}]_{dust}-[U_{238}]_{ice}}{[U_{234}]_{ice}^{in}-f\,[U_{238}]_{dust}-[U_{238}]_{ice}}\right) \quad (3)$$

A.2. Calculation of Density

The average density of the mineral dust was calculated based on literature modal mineralogies for Dome C (Table A1) from Gaudichet et al. (1986, 1988). Gaudichet et al. (1988) indicated that metallic oxides found in at least one Vostok sample originated from contamination. Given that the high density and non-aerodynamic shape of metallic oxides make their transport to the high plateau unlikely, we do not include these in the calculation. Average densities, using pure mineral density values for identified minerals (Table A1), range between 2.6 and 2.62 g/cm^3. More recently, Sala et al. (2008) also found talc and muscovite within Dome C ice. And, while no literature has presented direct evidence for carbonate in the Dome C ice, it is likely that previous procedures that melted ice without buffering the meltwater to neutral pH dissolved any carbonate. These three minerals, talc, muscovite, and carbonate, were incorporated into the density calculation by assigning the *Unidentified* modal percentages to these higher density minerals and result in an average density of 2.64 $\pm$ 0.052 (2 S.D.).

Table A1: Compiled Mineralogical Data

		Vostok*					Dome C*				
	Sample No.	1	2	3	4	5	1	2	3	4	5
	Depth(m)	125	475	925	1675	2025	246	552	580	678	838
	Age (ka)	5	24	60	122	150	6	16	18	36	50
	density g/cm^3	Relative abundances %									
Illite	2.6[a]	30	19	33	24	24	34	28	26	32	34
Kaolinite	2.61[a]	-	-	-	-	-	4	3	-	-	-
Chlorite	2.8[b]	-	6	5	-	4	-	3	4	5	6
Smectite	2.6[a]	7	3	13	5	6	-	-	6	-	-
Quartz	2.65[a]	14	15	7	8	8	-	23	12	13	8
Feldspars	2.58[a,c]	6	17	18	10	18	12	23	22	13	18
Pyroxenes, Amphiboles	3.1[a,d]	-	-	-	-	-	15	6	-	5	2
Amorph Si (opal)	2.07[a]	6	2	2	8	3	-	6	4	-	-
Metallic Oxides	3.5-4.5	12	3	1	11	1	4	-	-	-	-
Volcanic glass	2.38[e]	-	-	-	-	-	11	-	6	5	-
Colloidal		12	7	-	14	6	-	-	-	-	-
Ca Compounds		3	-	-	3	3	-	-	-	-	-
Unidentified		10	28	21	17	23	20	8	20	27	32
Muscovite	2.82[a]										
Talc	2.7[a]										
Calcite	2.71[a]										

Ice core data from Gaudichet et al. (1986, 1988). [a]Primary mineral data from Deer et al. (1996). [b] Average of multiple values in Holeman (1965). [c]Gaudichet et al. (1986) indicate primarily Ca and K feldspar (orthoclase and albite); Sala et al. (2008) found K-feldspar, therefore we use the average density of the two feldspars. [d]Gaudichet et al. (1986) do not distinguish between pyroxenes and amphiboles, Sala et al. (2008) did not find pyroxenes, only amphibole therefore we use the hornblende average. [e]Wada and Wada (1977)

A.3. BET nano-scale

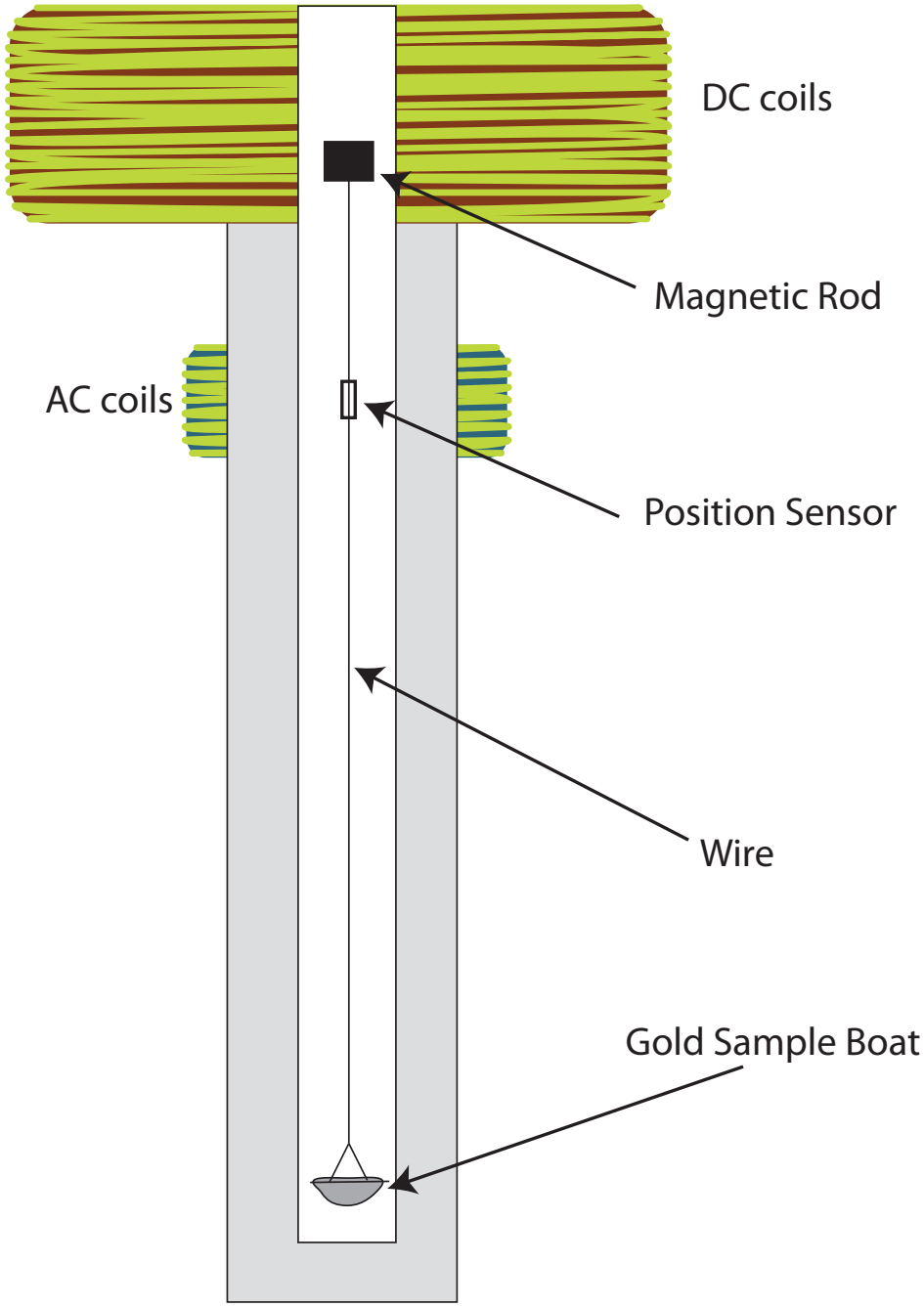

Figure A1: Schematic of the ETH nano scale.

A.4. Raw data

Data table includes concentrations of uranium, U, in ppt (ng/kg), the uranium activity ratio, ($^{234}U/^{238}U$); the radiogenic strontium, $^{87}Sr/^{86}Sr$, and neodymium, $^{143}Nd/^{144}Nd$, isotopic compositions; the surface area, S_{BET}, and fractal dimension, D, values measured using the BET nano-scale (see below for description); the calculated recoil factors, f, and ages for each sample. Three sets of sample ages are calculated. One set of samples was measured prior to the availability of the nano-scale BET (starred); these sample ages were calculated by assigning the f values measured on the samples from the same depth with an$f$ value error of 10%. These samples are noted in gray in Figure 2 of the main text. The second set of samples were measured using the initial set-up of the nano-scale BET (see discussion below), which provided some S_{BET} values with high errors; errors in the calculated ages are as high as 50%. The final set of samples were measured show lower errors in S_{BET} and correspondingly lower errors in the ages. Errors reported here are calculated based on a "bootstrap" Monte Carlo approach.

Table A2: Dome C Data*

Sample depth (m)	U ppt	2σ	$\left(^{234}U/^{238}U\right)$	2σ	$^{87}Sr/^{86}Sr$	2σ	$^{143}Nd/^{144}Nd$	2σ	S_{BET} m^2/g	2σ	D	2σ	f	2σ	age ka	2σ
112 (D)	0.033	10			n.d.		n.d.									
112 (I)	0.051	9	1.11	9	0.709081	100	n.d.									
990 (D)	1.092	7			0.709462	40	0.512394	30	29.98	1.29	2.355	0.044	0.1584	0.0081		
990 (I)	0.211	1	1.281	1	0.708778	40	0.512480	100							83	16
1040 (D)	0.794	2			0.710889	40	0.512512	25	n.m		n.m.					
1040 (I)	0.301	1	1.201	11	0.708845	40	0.512566	25							88*	35*
1900 (D)	1.454	7			0.709416	40	0.512453	25	n.m.		n.m.					
1900 (I)	0.414	2	1.389	13	0.708926	40	0.512513	25							256*	74*
1901 (D)	0.823	8			0.709754	40	0.512499	25	34.75	1.39	2.366	0.012	0.1776	0.0081		
1901 (I)	0.232	3	1.353	13	0.709072	40	0.512495	25							202	26
2603 (D)	1.459	7			0.709856	10	0.512521	25	35.62	1.44	2.348	0.025	0.1922	0.0090		
2603 (I)	0.544	3	1.359	12	0.708979	10	0.512569	100							311	48
2604 (D)	1.218	8			0.709661	40	0.512516	12	n.m.		n.m.					
2604 (I)	0.488	3	1.344	13	0.708603	40	0.512556	12							325*	154*
2812 (D)	1.142	5			0.709554	40	0.512422	25	48.06	1.98	2.395	0.022	0.2250	0.0084		
2812 (I)	0.392	3	1.498	13	0.709032	40	0.512491	50							421	65
2813 (D)	1.036	4			0.710107	100	0.512479	12	n.m.		n.m.					
2813 (I)	0.593	2	1.314	13	0.708931	100	0.512536	24							413*	310*
3218 (D)	1.007	5			0.709027	20	0.512448	16	48.84	0.49	2.552	0.013	0.1430	0.0034		
3218 (I)	0.261	3	1.498	14	0.708268	20	0.512552	20							723	191
3220 (D)	0.826	4			0.708944	40	0.512450	20	48.97	5.88	2.534	0.013	0.1512	0.0185		
3220 (I)	0.235	1	1.492	13	0.708205	30	0.512544	25							813	621
3245 (D)	0.622	3			0.709587	40	0.512464	12	52.97	5.27	2.573	0.013	0.1458	0.0148		
3245 (I)	0.179	1	1.475	14	0.708170	30	0.512581	100							870	624
3246 (D)	0.719	2			0.709110	100	0.512444	12	49.43	0.74	2.546	0.013	0.1473	0.0039		
3246 (I)	0.187	1	1.512	10	0.707973	40	0.512538	50							730	165
3255 (D)	4.372	22			0.708603	40	0.512461	24	53.15	0.85	2.577	0.007	0.1446	0.0039		
3255 (I)	0.419	2	1.421	14	0.708100	40	0.512564	20							82	6

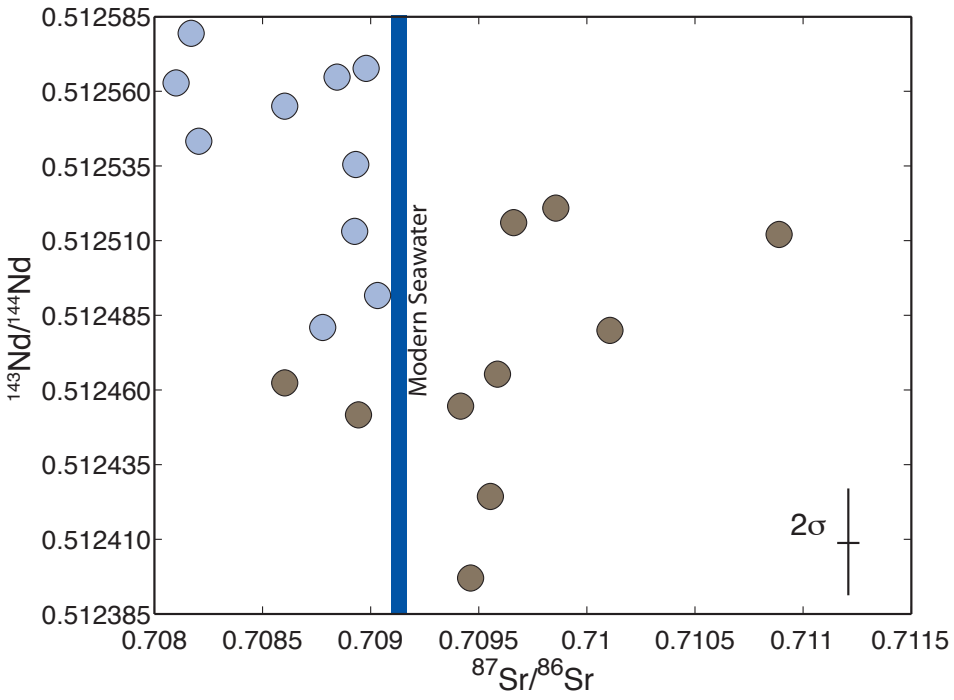

Figure A2: Dome C Sr and Nd isotopic compositions of dust (brown) and ice (blue). Also shown is the range of modern surface seawater values for Sr (constant) and Nd (variable).

A.5. Surface Areas from Mineralogy

Table A3: Compiled Surface Area Data

Mineral	Size Range (μm)	S_{BET}	Power Law Function
Illite[a]			$108.54*d^{-0.528}$
	< 2	119	
	< 2	99	
	< 63	13	
	< 63	25	
Kaolinite			$23.052*d^{-0.363}$
	< 2	19 [b]	
	< 2	47 [c]	
	0.2	35 [d]	
	0.25	30 [d]	
	0.45	39 [d]	
	0.86	20 [d]	
Chlorite[e]			$106.77*d^{-0.998}$
	63	1.71	
	200	0.54	
Smectite[b] (var Illite, Kaolinite)	< 2	180	
Quartz and Carbonate			$3*d^{-0.772}$
	< 2	3 [f]	
	50-125	0.1 [g]	
Feldspar - Amphibole Mixture[h]			$34.117*d^{-0.69}$
	15	8.46	
	60	1.12	
	100	1.23	
	200	0.77	
	350	0.68	
	750	0.46	
Amorph Si (opal) [i]			$144.47*d^{-0.579}$
	< 2 - 5	85	
	5-10	40	
Volcanic glass [j]			$1.655*d^{-0.174}$
	5	1.242	
	228	0.6713	
	842	.4896	
	4123	0.3938	
Muscovite [k]			$13.628*d^{-0.938}$
	0.5	29.5	
	1.5	7.12	
	3.75	4.57	
Talc			$10.76*d^{-1.032}$
	1	22 [l]	
	10	0.5 [m]	

[a]Uncles et al. (2006); [b]Omotoso and Mikula (2004); [c]Hughes et al. (2009); [d]Ormsby and Shartsis (1960); [e]Brandt et al. (2003); [f]Banin et al. (1975); [g]Gautier et al. (2001); [h]White et al. (1996); [i]Van Bennekom et al. (1991); [j]Bourcier et al. (2000); [k]Raman and Mortland (1966);[l] Holland and Murtagh (2001); [m]Ferrer et al. (2001)

Figure A3: Functions Describing Variations in S_{BET} with Grain Size. Red lines are the plotted power law functions for each mineral. Gray shaded area is the lognormal distribution of the grain size. S_{BET} is shown for each mineral.

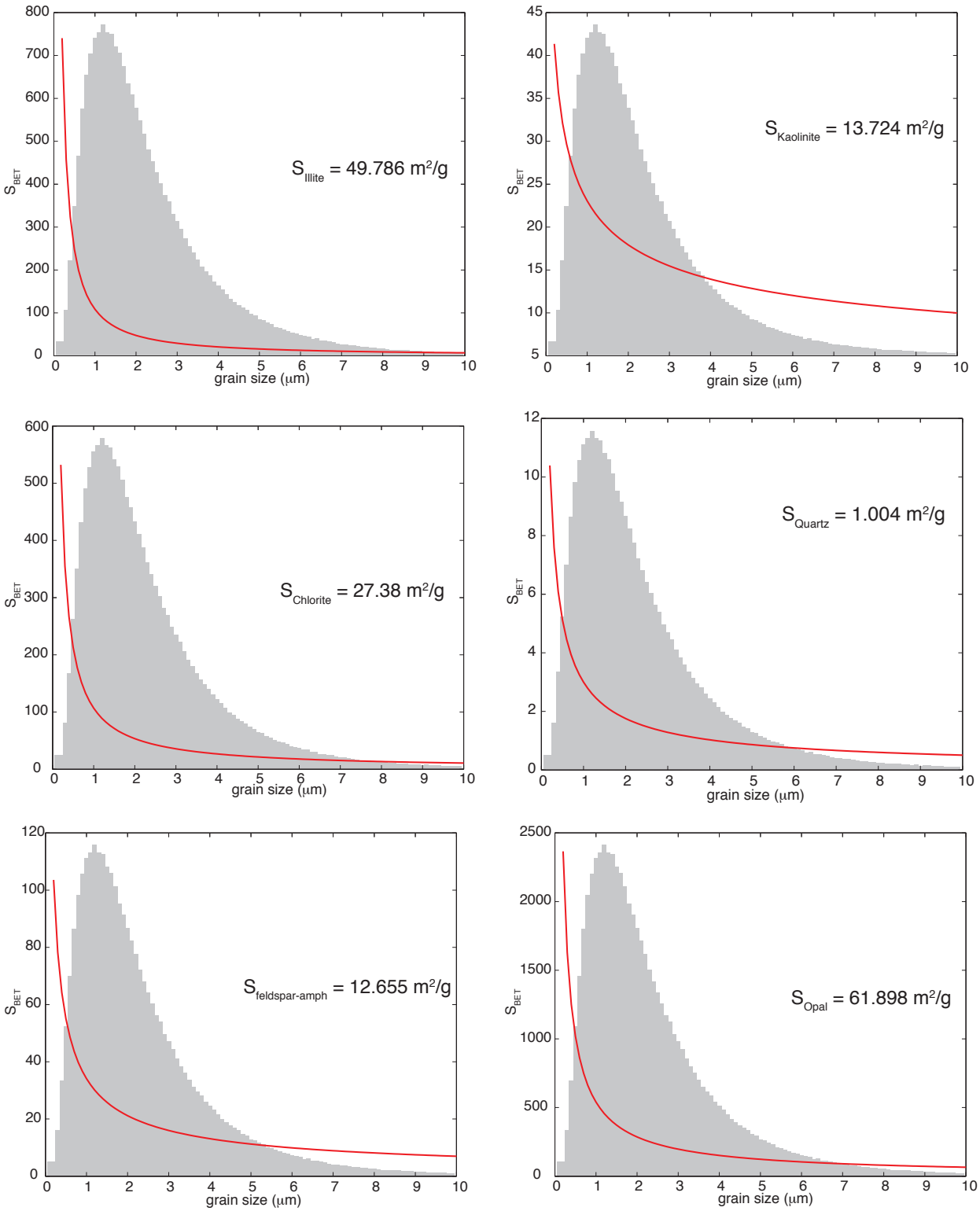

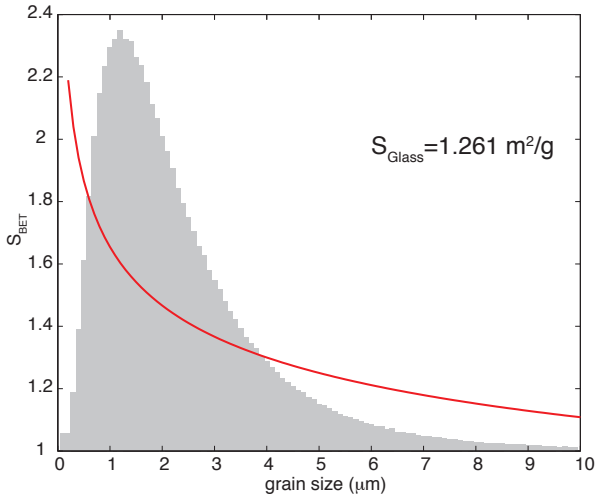
S_{Glass}=1.261 m²/g
S_{BET}
grain size (μm)

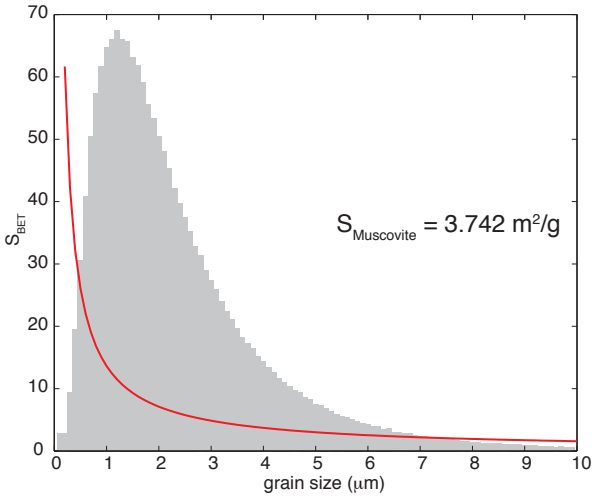
$S_{Muscovite}$ = 3.742 m²/g
S_{BET}
grain size (μm)

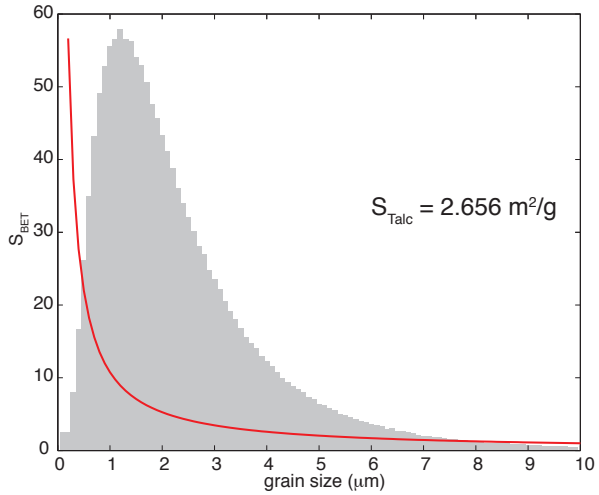
S_{Talc} = 2.656 m²/g
S_{BET}
grain size (μm)

A.6. Local bed topography at Dome C

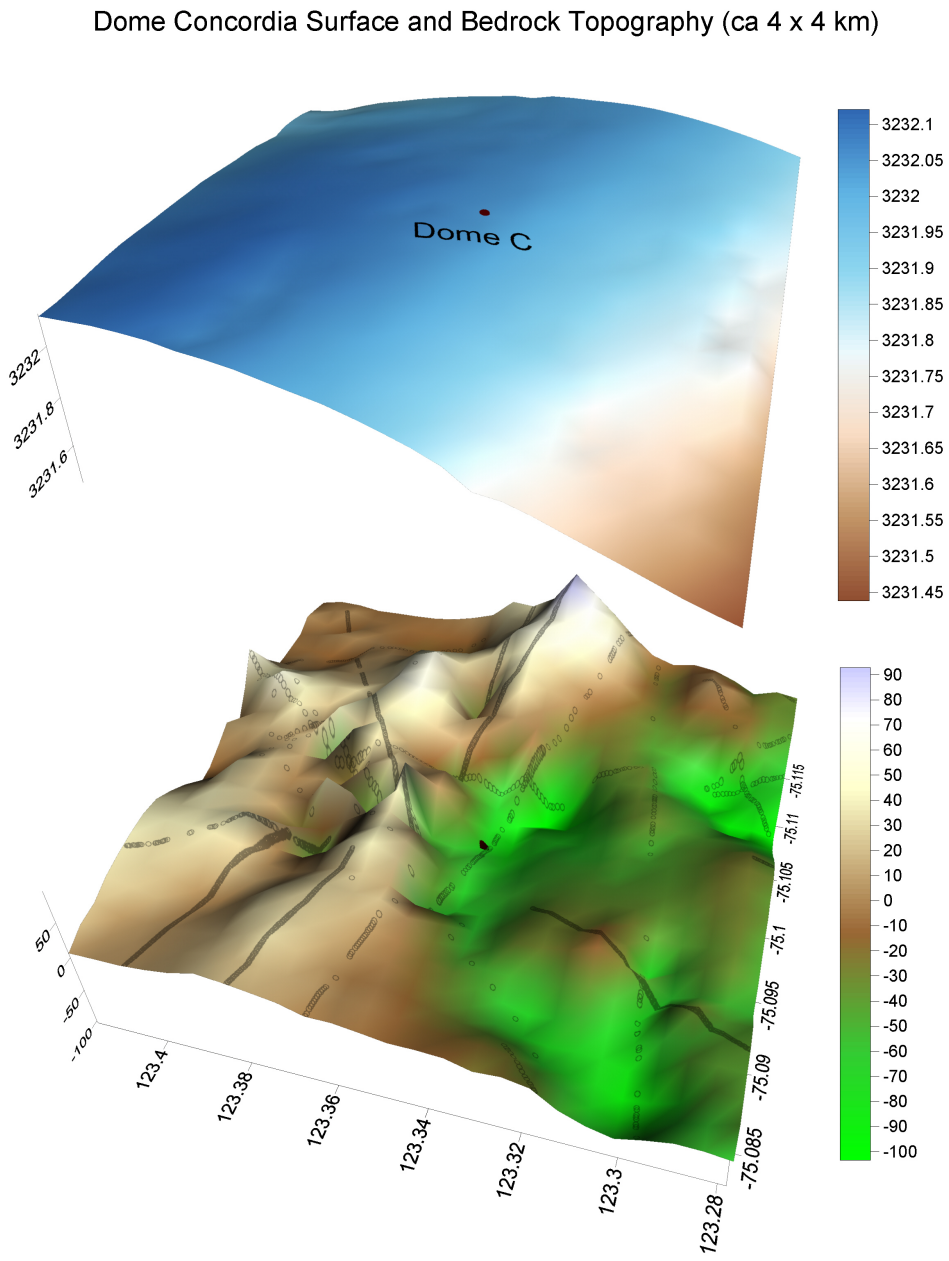

Figure A4: Local topography (m a.s.l.) around Dome Concordia. Bedrock elevations have been obtained by airborne and surface radar sounders (Forieri et al., 2005) (note that deviations of up to several 10 meters on an absolute scale are possible). The drilling site is marked by a dot in the center. All radar sounding positions used to generate the map are marked with grey circles. A 25x25 point grid has been interpolated with a Kriging method.

References

Banin, A., Gal, M., Zohar, Y., Singer, A., 1975. The specific surface area of clays in lake sediments-measurement and analysis of contributors in Lake Kinneret, Israel. Geochimica et Cosmochimica Acta 20, 278–282.

Bourcier, W.L., Roberts, S., Smith, D.K., Hulsey, S., Newton, L., Sawvel, A., Bruton, C., Papelis, C., Um, W., Russell, C.E., Chapman, J., 2000. Determination of Reactive Surface Area of Melt Glass. Technical Report UCRL-ID-145181. Lawrence Livermore National Lab., CA (US).

Brandt, F., Bosbach, D., Krawczyk-Brsch, E., Arnold, T., Bernhard, G., 2003. Chlorite dissolution in the acid ph-range: a combined microscopic and macroscopic approach. Geochimica et Cosmochimica Acta 67, 1451–1461.

Deer, W., Howie, R., Zussman, J., 1996. An Introduction to the Rock-Forming Minerals. Prentice Hall. 2 edition.

Dickin, A.P., 2005. Radiogenic Isotope Geology. Cambridge University Press. 2 edition.

Faure, G., Mensing, T.M., 2004. Isotopes: Principles and Applications. Wiley. 3 edition.

Ferrer, J., Villarino, M.A., Tura, J.M., Traveria, A., Light, R.W., 2001. Talc preparations used for pleurodesis vary markedly from one preparation to another. Chest Journal 119, 1901–1905.

Fireman, E., 1986. Uranium series dating of Allan Hills ice. Journal of Geophysical Research-Solid Earth and Planets 91, D539–D544.

Forieri, A., Zuccoli, L., Bini, A., Zirizzotti, A., Remy, F., Tabacco, I., 2005. New bedrock map of Dome C, Antarctica, and morphostructural interpretation of the area. Annals of Glaciology 39, 321–325.

Gaudichet, A., De Angelis, M., Lefevre, R., Petit, J.R., Korotkevitch, Y., Petrov, V., 1988. Mineralogy of Insoluble Particles in the Vostok Antarctic Ice Core Over the Last Climatic Cycle(150 kyr). Geophysical Research Letters 15, 1471–1474.

Gaudichet, A., Petit, J.R., Lefevre, R., Lorius, C., 1986. An investigation by analytical transmission electron microscopy of individual insoluble microparticles from Antarctic (Dome C) ice core samples. Tellus 38B, 250–261.

Gautier, J., Oelkers, E., Schott, J., 2001. Are quartz dissolution rates proportional to BET surface areas? Geochimica et Cosmochimica Acta 65, 1059–1070.

Holeman, J., 1965. Clay Minerals. Technical Report 28. U.S. Department of Agriculture; Soil Conservation Service, Engineering Division.

Holland, H., Murtagh, M., 2001. An XRD morphology index for talcs: The effect of particle size and morphology on the specific surface area, Advances in X-ray Analysis. pp. 421–428.

Hughes, J., Gilkes, R., Hart, R., 2009. Intercalation of reference and soil kaolins in relation to physico-chemical and structural properties. Applied Clay Science 45, 24–35.

Lee, V.E., DePaolo, D.J., Christensen, J.N., 2010. Uranium-series comminution ages of continental sediments: Case study of a pleistocene alluvial fan. Earth and Planetary Science Letters 296, 244–254.

Omotoso, O., Mikula, R., 2004. High surface areas caused by smectitic interstratification of kaolinite and illite in Athabasca oil sands. Applied Clay Science 25, 37–47.

Ormsby, W., Shartsis, J., 1960. Surface area and exchange capacity relation in a Florida kaolinite. Journal of the American Ceramic Society 43.

Raman, K., Mortland, M., 1966. External specific surface area and vermiculite. The American Mineralogist 51.

Sala, M., Dapiaggi, M., Delmonte, B., Artioli, G., Marino, F., Maggi, V., Petit, J.R., 2008. First mineralogical and crystallographic results on dust from the EPICA Dome C ice core, EGU.

Uncles, R., Stephens, J., Harris, C., 2006. Properties of suspended sediment in the estuarine turbidity maximum of the highly turbid Humber Estuary system, UK. Ocean Dynamics 56, 235–247.

Van Bennekom, A., Buma, A., Nolting, R., 1991. Dissolved aluminium in the Weddell-Scotia Confluence and effect of Al on the dissolution kinetics ofbiogenic silica. Marine Chemistry 35, 423–434.

Wada, S.I., Wada, K., 1977. Density and structure of allophane. Clay Minerals 12, 289–298.

White, A., Blum, A., Schulz, M., Bullen, T., Harden, J., Peterson, M.L., 1996. Chemical weathering rates of a soil chronosequence on granitic alluvium: I. Quantification of mineralogical and surface area changes and calculation of primary silicate reaction rates. Geochimica et Cosmochimica Acta 60, 2533–2550.